# Limiting-law excess sum rule for polyelectrolytes

Jonathan Landy,[1,*] YongJin Lee,[2,3] and YongSeok Jho[2,3,†]

[1] *Materials Department, University of California, Santa Barbara, CA 93106, USA*
[2] *Department of Physics, POSTECH, Pohang 790-784, South Korea*
[3] *Asia-Pacific Center for Theoretical Physics, Pohang, 790-784, South Korea*

(Dated: November 12, 2013)

We revisit the mean-field limiting-law screening excess sum rule that holds for rod-like polyelectrolytes. We present a new, efficient derivation of this law that clarifies its region of applicability: The law holds in the limit of small polymer radius, measured relative to the Debye screening length. From the limiting-law, we determine the individual ion excess values for single-salt electrolytes. We also consider the mean-field excess sum away from the limiting region, and we relate this quantity to the osmotic pressure of a dilute polyelectrolyte solution. Finally, we consider numerical simulations of many-body polymer-electrolyte solutions. We conclude that the limiting-law often accurately describes the screening of physical charged polymers of interest, such as extended DNA.

PACS numbers: 82.35.Rs, 61.20.Qg, 87.14.Gg

## I. INTRODUCTION

The *excess* of a particular species of ion provides a measure of the number of molecules of that species taking part in the screening of a charged source within an electrolyte – *cf.* (3) below [1]. Recently, thermodynamic arguments have been exploited to allow for changes in excess with applied force to be inferred from single-molecule force-extension data [2–9]. In principle, these new measures could provide a valuable metric for characterizing competing states. However, excess differences between states can only arise through non-linear screening mechanisms [10], and extraction of the full information contained in these measures (*e.g.,* regarding local structure) provides a theoretical challenge.

Ramanathan has presented one of the few general analytic results relating to ionic excess values: Under certain conditions, the mean-field excess sum associated with the screening of a rod-like polyelectrolyte approaches a fixed, universal value, independent of electrolyte composition [11]. In this paper, we provide a new derivation of this limiting-law that relies only upon simple thermodynamic and scaling arguments. This approach avoids technical analysis of the Poisson-Boltzmann equation, and it also leads to a clarification of the law's region of applicability: The limiting-law holds only in the limit of $\kappa a \to 0$, with $\kappa$ the inverse Debye length and $a$ the rod's radius. Away from the limiting region, we show that the excess sum decreases as the unitless quantity $\kappa a$ increases. We obtain a good approximation to this $\kappa a$ dependence that holds for polymers that are not too highly charged; for highly charged polymers, or high valence electrolytes, the $\kappa a$ dependence takes on a non-universal functional form. Finally, we report on simulations of full, many-body polymer-electrolyte systems. These show good agreement with the mean-field results. Thus, our mean-field estimates of the excess in the rod-like geometry can often be used in conjunction with experimental differential-excess data, such as that of [9], to obtain accurate estimates of the net excess in general conformational states for polyelectrolytes.

In the following section we present our new proof of the limiting-law, and discuss consequences. In section III, we consider the behavior at finite $\kappa a$: There, we discuss, among other things, simulations of model systems, including models for extended DNA. In section IV, we conclude with a brief discussion of our results.

## II. LIMITING-LAW

### *Derivation*

As depicted in Fig. 1, we consider the screening of a uniformly charged cylindrical rod of length $L \gg a, \kappa^{-1}$ and linear charge density $\lambda$ ($\equiv e/b$). We take the rod to

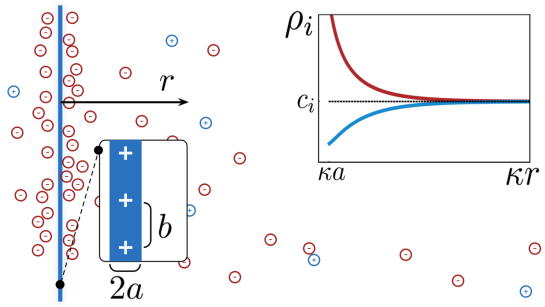


FIG. 1: (color online) A screened, uniformly charged rod. Inset: Plot of average number density $\rho_i$ versus distance from the rod for both counter- and co-ions (monovalent, single-salt case shown). The excess $n_i$, defined in (3), is approximately equal to the integral of $\rho_i - c_i$ over the volume.

*Electronic address: landy@mrl.ucsb.edu
†Electronic address: ysjho@apctp.org

sit within a large, bulk electrolyte of volume $V$, which can formally be taken to infinity. The partition sum for a cylindrical volume of radius $R \gg a$, coaxial with the rod is then formally,

$$\mathcal{Z} = \sum_{\{N_j\}} e^{-\beta\left[F_{\rm int}(\{N_j\}) - \sum_i \mu_i N_i\right]}, \tag{1}$$

where $N_j$ is the number of molecules of species $j$ within the volume, $\mu_j$ is its chemical potential (held fixed by the bath at infinity), and $F_{\rm int}(\{N_j\})$ is the free energy at fixed $\{N_j\}$. Working at constant temperature and pressure, variations in the chemical potentials are interrelated through the bulk's Gibbs-Duhem relation $\sum_i c_i d\mu_i = 0$ [1]. Solving for the variation of the solvent's chemical potential $\mu_W$ (water, perhaps) in terms of the variations of those of the solutes gives for the variation of $\mathcal{F} \equiv -T\log\mathcal{Z}$, the free energy of the volume,

$$d\mathcal{F} = L\phi(a)d\lambda - \sum_i \langle n_i\rangle d\mu_i. \tag{2}$$

Here, $\phi$ is the electrostatic potential, the sum is over solute species only, and $n_i$, the *excess of species* $i$, is

$$\begin{aligned} n_i &= \lim_{R\to\infty} N_i - \frac{c_i}{c_w}N_w \\ &= \lim_{R\to\infty} N_i - c_i\overline{V} - \frac{c_i}{c_W}\{N_W - c_W\overline{V}\}. \end{aligned} \tag{3}$$

In this last line above, $\overline{V} \propto R^2 - a^2$ is the volume accessible to the solution and $c_i \equiv c\bar{c}_i$ is the bulk concentration of solute species $i$, with $c$ some reference concentration scale. We work here under the dilute assumption, so that $\mu_i \approx T\log c_i$. In this case, the bracketed term in the bottom line of (3) can be neglected, and $n_i$ is approximately equal to the total number of molecules of species $i$ near the rod, minus the number that would be present if the solution resembled the bulk throughout.

We take for now the mean-field approximation, and suppose that the dimensionless potential $y \equiv e\phi/T$ satisfies the Poisson-Boltzmann equation [12],

$$\nabla^2 y = -4\pi l_B \sum_i q_i c_i e^{-q_i y}, \tag{4}$$

where $l_B = \frac{e^2}{\epsilon T}$ is the Bjerrum length, the sum is over the present ion species, and the $q_i$ are their integer valences [29]. For a general source distribution sitting in a bulk electrolyte, the corresponding mean-field approximation to the excess of species $i$ associated with the source is given by the formal expression

$$n_i = c_i \int_{\overline{V}} \left(e^{-q_i\phi(\mathbf{r})/T} - 1\right) d^3r. \tag{5}$$

In cylindrical coordinates the boundary conditions on $y$ for the cylindrical geometry are

$$\begin{aligned} \lim_{r\to a} r\partial_r y &= -2\xi, \\ \lim_{r\to\infty} y &= 0, \end{aligned} \tag{6}$$

where $\xi = l_B/b$ is a dimensionless measure of the charge density of the line. Setting $\mathbf{r}' = \kappa\mathbf{r} \equiv \mathbf{r}\times\sqrt{4\pi l_B c\sum_i \bar{c}_i q_i^2}$ gives a new system of equations for $y$, in which the only $c$-dependence appears in the inner boundary position, $a' \equiv \kappa a$. The potential therefore takes the scaling form

$$\phi \equiv \frac{T}{e} y(\kappa r; \kappa a; \xi; \{q_i, \bar{c}_i\}), \tag{7}$$

in the original coordinates.

Recalling that $\mu_i = T\log(c\bar{c}_i)$, equating the mixed partials of (2) gives the Maxwell relation

$$\begin{aligned} \frac{T}{c}\partial_\lambda \sum_i n_i/L &= -\partial_c\phi(r)|_a \\ &= -\frac{1}{2c}\left\{r\partial_r\phi(r) + a\partial_a\phi(r)\right\}|_a, \end{aligned} \tag{8}$$

where (7) has been used in the second line to re-express the derivative with respect to $c$ in the first [30]. For thin lines, the second term on the right side above is zero, and the first term on the right can be evaluated through the use of the first boundary condition in (6). Integrating with respect to $\lambda$ (using the fact that the effective line charge density is constant above the critical, bare Manning-threshold value [13, 14]) then gives

$$\sum_i \overline{n}_i = \begin{cases} \frac{1}{2}\xi^2, & \xi < |q_M|^{-1} \\ \left(\frac{|q_M\xi| - \frac{1}{2}}{q_M^2}\right), & \xi > |q_M|^{-1}, \end{cases} \tag{9}$$

where $q_M$ is the valence of the strongest counterion present (that which condenses onto the line above the Manning threshold), and $\overline{n}_i \equiv (l_B/L)n_i$. The result (9) is the universal, mean-field limiting-law sum rule for rod-like polyelectrolytes: It holds for any electrolyte, provided the system is in the excess-salt, low ionic strength limit [31]. As noted above, Ramanathan arrived at this result previously through an impressive, technical analysis of the Poisson-Boltzmann equation. However, only a proof outline was given in [11], and this did not make explicit that (9) holds only in the $\kappa a \to 0$ limit.

### *Applications*

We now discuss two immediate applications of (9). First, we note that for a single-salt electrolyte, (9) can be used to determine the two individual ion species excesses: If the negative species of ion has valence and concentration $(-q_-, q_+c)$ and the positive species has valence and concentration $(q_+, q_-c)$, local charge neutrality near the macromolecule requires $\xi - q_-\overline{n}_- + q_+\overline{n}_+ = 0$. For $\xi > 0$, solving with (9) gives

$$\begin{aligned} \overline{n}_- &= \frac{\xi}{q_+ + q_-}\left\{1 + \frac{q_+\xi}{2}\right\} \\ \overline{n}_+ &= -\frac{\xi}{q_+ + q_-}\left\{1 - \frac{q_-\xi}{2}\right\}, \quad \xi < q_-^{-1}, \end{aligned} \tag{10}$$

below threshold, and

$$\begin{aligned}\overline{n}_- &= \frac{\xi - q_-^{-1}}{q_-} + \frac{1}{2q_-^2} + \frac{1}{2q_-(q_+ + q_-)} \\ \overline{n}_+ &= -\frac{1}{2q_-(q_+ + q_-)}, \quad \xi > q_-^{-1}, \end{aligned} \tag{11}$$

above threshold. These expressions agree with the 1-1 results of [13, 15–17] (obtained through various approximate means), as well as with the 1-1 and 2-1 subthreshold expressions of [18] (obtained rigorously via connection to Fredholm-determinant theory). While the sum rule (9) holds for any electrolyte composition, we note that a two term expansion for the individual excesses will not hold in general as it does in the single-salt case (as in (10) and (11), which are quadratic and linear in $\xi$, respectively). This can be demonstrated through direct expansion of the $\{n_i\}$, using the methods of [10, 19].

Second, we note that upon integrating the Maxwell relation (8) with respect to both $\lambda$ and $c$, we obtain

$$\begin{aligned} L\int_0^\lambda \phi(r;\lambda')|_a \, d\lambda' &= -T\log c \sum_i n_i + \mathcal{F}_0(\{q_j, \overline{c}_j\}, \lambda, T) \\ &= \mathcal{F}. \end{aligned} \tag{12}$$

Here, we have used the fact that the excess sum is independent of $c$ for thin lines and $\mathcal{F}_0$ is a $c-$independent integration constant [32]. We now consider a large volume $V$ consisting of $N_M$ thin lines (with $c_M \equiv N_M/V \ll L^{-3}$), in contact via water-permeable membrane with an exterior solute-free bath solution. Adding together the free energy of the solute, the free energy of charging (12) for each of the $N_M$ lines, and finally the configuration entropy of the lines, differentiating with respect to $V$ we obtain for the osmotic pressure $\Pi$ of the volume,

$$\frac{\Pi V}{T} = \sum_i N_i + N_M\left(1 - \sum_i n_i\right), \tag{13}$$

with $n_i$ the excess per line. The last term above provides a correction to the ideal gas law that reflects the fact that a macromolecule and its screening cloud act as a single composite object, contributing only one $TV^{-1}$ to the osmotic pressure of a solution. Although we have derived (13) here by making use of results that hold for thin lines only, this relationship between the osmotic pressure and the excess sum actually holds for general geometries [20]. Plugging (9) into (13) we obtain an estimate for the osmotic pressure of a dilute polyelectrolyte solution – a result that is also discussed in [21].

## III. BEHAVIOR AT FINITE RADIUS

At finite $a$, it follows from (7) and (8) that the mean-field excess sum develops a $c$ dependence through the quantity $\kappa a \propto \sqrt{c}a$ (with no other independent dependence on either $c$ or $a$ appearing in the sum). Exact analytic results relating to this dependence are difficult to obtain. To gain insight, we turn now to a consideration of numerical solutions to (4) and also non-mean-field simulation results. We obtained numerical solutions to (4) using the 1D finite difference method and the Newton-Raphson scheme. We performed extensive Monte Carlo simulations based on the primitive model, using MMM1D to evaluate charge interactions [22], with enforced periodic boundary conditions along the axial direction in order to mimic an infinitely long line charge (period 22nm). We set the radius of the cylinder to $a = 2$Å and the radius of the free ions to 1Å, both small values in order to reduce steric effects. We took $10^5$ steps for equilibration, and averaged over $10^6$ steps to obtain equilibrium charge density profile estimates. Further, for each data point, we ran three independent simulations in order to obtain variance estimates.

Data representative of our numerical results are presented in Fig. 2. In Fig. 2a, numerically integrated excess sums for (4) are plotted against $\xi$ for both 1-1 and 2-1 salts for the thin line geometry. These are in agreement with the analytic values (9), up to small errors above threshold, likely due to the imperfect condensate characterization that results from discretization of (4). In Fig. 2b, we plot the excess sum from (4) against $\kappa a$ for $\xi = 1.0$. In this case, the 1-1 salt is at threshold, while the 2-1 salt is above. They thus approach differing $\kappa a \to 0$ values; our numerical checks and previous analytic work [23] both suggest that this approach is continuous. We have also plotted in Fig. 2b a second order expansion for the sum, obtained using the methods of [10, 19]. This is,

$$\lim_{\kappa a\to\infty||\lambda\to 0}\sum_i \overline{n}_i \sim \frac{1}{2}\xi^2\left[1 - \left(\frac{K_0(\kappa a)}{K_1(\kappa a)}\right)^2\right], \tag{14}$$

where the $K_i$ are modified Bessel functions [33]. Notice that (14), which one would naively expect to hold only at large $\kappa a$ (where the source charge density is weak and the expansion converges quickly for all $\xi$), is actually exact at $\kappa a = 0$, below the Manning threshold. Consequently, as shown in Fig. 2b, the approximation (14) provides a quantitatively accurate approximation at most $\kappa a$, below threshold. One can also use (14) to estimate the sum above threshold (replacing $\frac{1}{2}\xi^2$ in (14) with $\left(\frac{|q_M\xi|-\frac{1}{2}}{q_M^2}\right)$ – the super-threshold limiting-law sum value), provided $\xi$ is not too large: *e.g.*, this was done to obtain the solid curves in Fig. 2b. As an application, consider the case of single-stranded DNA at physiological salt concentrations, where $2a \approx \kappa^{-1} \approx 1$nm. The excess sum here is roughly $\sum_i \overline{n}_i \approx \left(\frac{|q_M\xi|-\frac{1}{2}}{q_M^2}\right) \times [1 - (\frac{K_0(0.5)}{K_1(0.5)})^2] \approx \left(\frac{|q_M\xi|-\frac{1}{2}}{q_M^2}\right) \times 0.7$, with $\xi \approx 2.1$ – that is, under physiological conditions, the sum is roughly three quarters its limiting-law value. Plugging this into (13) gives a finite-salt approximation for the osmotic pressure of a dilute single-stranded DNA solution. Further, using the charge-neutrality condition, this form can also be used to obtain estimates for the individual ion excess values, in single-salt solution.

In Fig. 2c we plot a snapshot of the simulated (non-

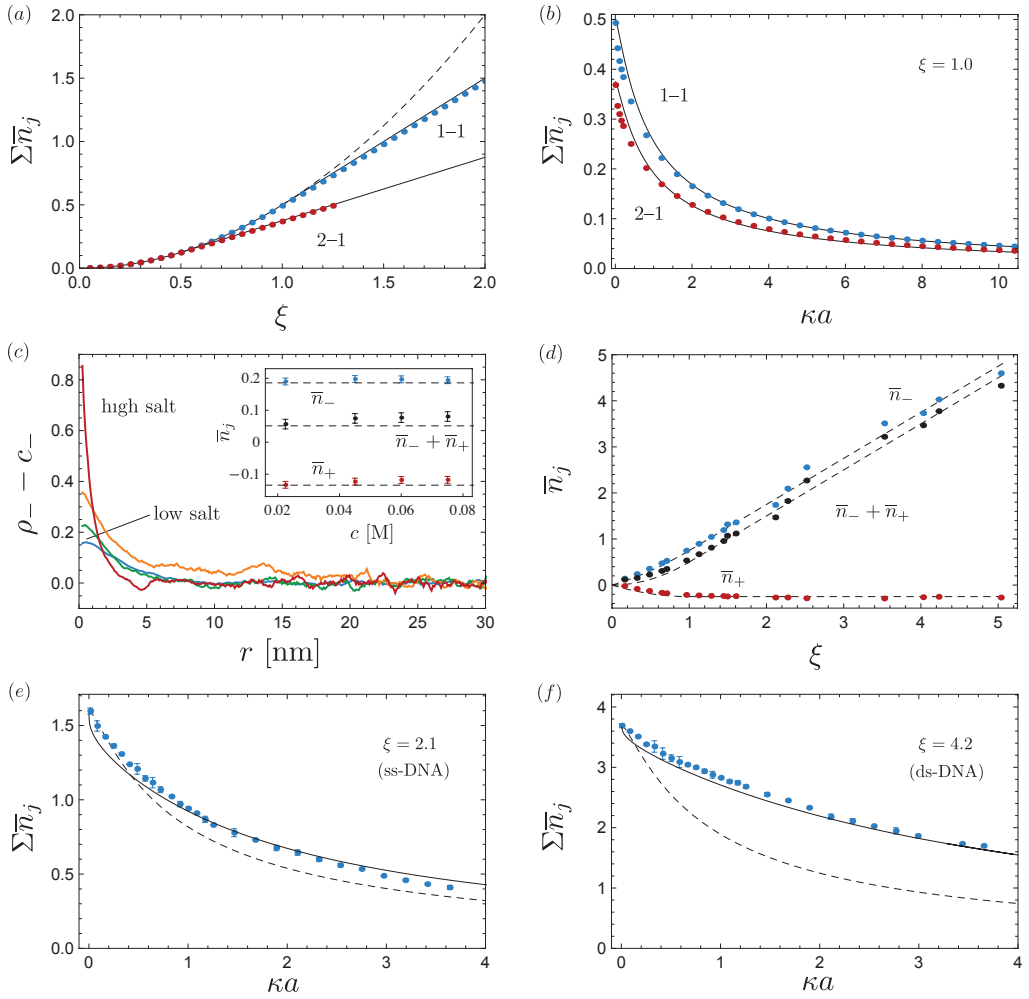


FIG. 2: (color online) Numerical Poisson-Boltzmann (*a,b*) and Monte Carlo simulation (*c,d,e,f*) results (length scales as noted in text). (*a*) Excess sum vs. $\xi$ at $a = 0$ for 1–1 and 2–1 salts: numerical (dotted), values from (9) (solid), and an extended quadratic form (dashed). (*b*) Excess sum vs. $\kappa a$ at $\xi = 1.0$ for 1–1 (at threshold) and 2–1 (above threshold) salts: numerical (dotted), approximate analytic form (14) (solid). (*c*) Snapshot excess counterion density vs. $r$ at $\xi = 0.32$ for four 1–1 salt concentrations. Inset shows net excess vs. $c$ for these four concentrations together with values from (9), (10) (dashed). (*d*) 1–1 salt, excess vs. $\xi$ at $c = 7.5$ mM: simulation values (dotted), values from (9–11) (dashed). (*e,f*) Excess sum vs. $\kappa a$ at $\xi = 2.1$ and 4.2 – values corresponding to single- and double-stranded DNA, respectively: simulation (dotted), numerical Poisson-Boltzmann (solid), and approximate form (14) (dashed). The approximation (14) performs well only at small to moderate values of $\xi$.

mean-field) counterion density as a function of radius for four salt concentrations. An inset shows the integrated excess for each of these four concentrations. Although the charge density profiles differ significantly across salt concentrations, the integrated sums show only a weak concentration dependence, in qualitative agreement with (9) and (10), which have no salt concentration dependence (for the concentrations shown here, $\kappa a$ is small in each case). In Fig. 2d, we plot the simulated excess totals versus $\xi$ at a fixed, small salt concentration. This again shows qualitative (and often quantitative) consistency with (9–11), even at high $\xi$. Finally, in Figs. 2e and 2f, we plot the excess sum versus $\kappa a$ for $\xi = 2.1$ and 4.2 – relatively large values approximating those of single- and double-stranded DNA, respectively. The solid lines in these figures are numerical Poisson-Boltzmann values, while the dashed lines are approximations from (14). As $\kappa a \to 0$, the excess sums approach values consistent with (9–11) in both cases. At finite $\kappa a$, the approximate form performs reasonably well for single-stranded DNA, but performs poorly for the double-stranded DNA model. Evidently, (9–11) can be expected to provide accurate excess sum estimates in the $\kappa a \to 0$ limit for many physical systems (even those with high charge density), while (14) provides an accurate, analytic approximation to the finite $\kappa a$ excess sum only for small to moderately charged ($\xi \lesssim 2$) systems.

## IV. DISCUSSION

To summarize, we have considered the excess sum associated with an isolated, rod-like polyelectrolyte. Ramanathan's prior derivation of the sum rule (9) made use of a contact identity relating the excess sum to the local ion number density at a polymer's surface [11, 16]. Working backwards from the limiting-law, the contact identity of [16] implies that the ion number density at the polymer's surface also approaches a universal limiting value for rod-like polymers (the two statements are equivalent). Thus, our derivation of the limiting-law also provides an efficient proof of this other result. Many other interesting results can also be derived efficiently using our approach. For example, at large $r$ it is known that the potential due to a polymer takes the form $\phi \sim 2\lambda_{eff} K_0(\kappa r)$, with $\lambda_{eff}$ a constant coefficient often referred to as the line's effective charge [21]. From (7), we see immediately that $\lambda_{eff}$ must be independent of $c$ – a result that is consistent with known exact results in the 1-1 salt case [17, 21].

Away from the limiting-region, our simulations show good agreement with the mean-field results, even at high charge densities, for monovalent salts. This suggests that the limiting-law often accurately characterizes physical systems. We intend to carry out further simulation tests, varying ion sizes and valences – two quantities that often directly control divergences from mean-field behavior [24, 25] – in the near-future.

### Acknowledgments

We thank P. Pincus, D. B. McIntosh, O. A. Saleh, M. Deserno, and G. S. Manning for helpful comments and J. Tecarro for producing Fig. 1. We also thank a referee for bringing to our attention the prior work of Ramanathan [11]. This work was partially funded by a grant from the USA NSF: Grant No. DMR-1101900. YJL and YSJ were partially supported by the Korean National Research Foundation: Grant Nos. NRF-2012R1A1A2009275.

[1] V. A. Parsegian, R. P. Rand, and D. C. Rau, Proc. Natl. Acad. Sci. USA **97**, 3987 (2000).
[2] D. E. Draper, RNA **10**, 335 (2004).
[3] H. Zhang and J. F. Marko, Phys. Rev. E **77**, 031916 (2008).
[4] B. A. Todd and D. C. Rau, Nucl. Acids Res. **36**, 501 (2007).
[5] B. Xiao, R. C. Johnson, and J. F. Marko, Nucl. Acids Res. **38**, 6176 (2010).
[6] P. Liebesny, S. Goyal, D. Dunlap, F. Family, and L. Finzi, J. Phys. Condens. Matter **22**, 414104 (2010).
[7] B. Xiao, H. Zhang, R. C. Johnson, and J. F. Marko, Nucl. Acids Res. **39**, 5568 (2011).
[8] S. Goyal, C. Fountain, D. Dunlap, F. Family, and L. Finzi, Phys. Rev. E **86**, 011905 (2012).
[9] J. Landy, D. B. McIntosh, and O. A. Saleh, Phys. Rev. Lett. **109**, 048301 (2012).
[10] J. Landy, D. B. McIntosh, O. A. Saleh, and P. Pincus, Soft Matter **8**, 9368 (2012).
[11] G. Ramanathan, J. Chem. Phys. **85**, 2957 (1986).
[12] P. M. Chaikin and T. C. Lubensky, *Principles of Condensed Matter Physics* (Cambridge University Press, 1995).
[13] G. S. Manning, J. Chem. Phys. **51**, 924 (1969).
[14] M. A. Lampert and R. S. Crandall, Chem. Phys. Lett. **72**, 481 (1980).
[15] L. M. Gross and U. P. Strauss, in *Chemical physics of ionic solutions*, edited by B. E. Conway and R. G. Barradas (Wiley, New York, 1966), p. 361.
[16] C. F. Anderson and M. T. Record, Jr., Biophys. Chem. **11**, 353 (1980).
[17] J. S. McCaskill and E. D. Fackerell, J. Chem. Soc. Faraday Trans. 2 **84**, 161 (1988).
[18] C. A. Tracy and H. Widom, Physica A **244**, 402 (1997).
[19] J. Landy, Phys. Rev. E **81**, 011401 (2010).
[20] R. A. Marcus, J. Chem. Phys. **23**, 1057 (1955).
[21] Y. Burak, Ph.D. thesis, Tel Aviv University (2004).
[22] A. Arnold and C. Holm, J. Chem. Phys. **123**, 144103 (2005).
[23] B. O'Shaughnessy and Q. Yang, Phys. Rev. Lett. **94**, 048302 (2005).
[24] T. Nishio and A. Minakata, J. Chem. Phys. **113**, 10784 (2000).
[25] T. Nishio and A. Minakata, J. Phys. Chem. B **107**, 8140 (2003).
[26] C. F. Wu, S. H. Chen, L. B. Shih, and J. S. Lin, Phys. Rev. Lett. **61**, 645 (1988).
[27] R. Das, T. T. Mills, L. W. Kwok, G. S. Maskel, I. S. Millett, S. Doniach, K. D. Finkelstein, D. Herschlag, and L. Pollack, Phys. Rev. Lett. **90**, 188103 (2003).
[28] G. S. Manning, J. Chem. Phys. **51**, 3249 (1969).
[29] Mean-field theory should work well even for highly-charged polymers provided the screening ions have concentrations and valences that are not too large. Its accuracy has been experimentally confirmed for various monovalent and divalent electrolyte solutions [26, 27].
[30] An exact identity similar to the first line of (8) will hold for any macromolecule. However, the simplified, second line of (8) is a consequence of the mean-field scaling form (7), which is special to the thin-line geometry. This scaling form may not hold outside of mean-field theory: *E.g.*, a $\kappa l_B$ dependence may enter into the potential, *etc.*
[31] The mean-field treatment here is self-consistent (*cf.* [12] for relevant discussion) in that it predicts zero fluctuations for the excess sum: *E.g.,* combining (1), (2), and (9), linear response gives $\langle(\sum_i n_i)^2\rangle - \langle\sum_i n_i\rangle^2 \propto \frac{\partial\langle\sum_i n_i\rangle}{T\partial \log c} = 0$. This last equality follows from the $c$-independence of the sum, which is a feature peculiar to the thin line geometry.
[32] The $\log c$ dependence in the free energy was first shown to hold by Manning through a Mayer ring expansion [28]. We see here that the proportionality constant is the excess sum. This term is part of that provided by the bath.
[33] At large $\kappa a$, (14) goes to zero scaling as $(\kappa a)^{-2}$.